学位論文　博士（医学）甲

Deficiency of BMAL1 promotes ROS generation and enhances IgE-dependent degranulation in mast cells

（BMAL1 の欠失はマスト細胞の ROS 産生を増加させ IgE による脱顆粒反応を亢進させる）

長坂　優香

山梨大学

Abstract

Background

Bmal1 (*Brain and muscle arnt-like,* or *Arntl*) is a bHLH/PAS domain transcription factor central to the transcription/translation feedback loop of the circadian clock. Mast cells are crucial for effector functions in allergic reaction and their activity follows a circadian rhythm. However, the functional roles of *Bmal1* in mast cells remain to be determined.

Purpose

This study aimed to elucidate the specific roles of *Bmal1* in IgE-dependent mast cell degranulation.

Results

IgE-dependent degranulation was enhanced in bone marrow–derived mast cells (BMMCs) derived from *Bmal1*-deficient mice (*Bmal1*-KO mice) compared to that in BMMCs derived from wild-type mice (WT mice) in the absence of 2-Mercaptoethanol (2-ME) in culture. Mast cell–deficient $Kit^{W\text{-}sh}$ mice reconstituted with *Bmal1*-KO BMMCs showed more robust passive cutaneous anaphylactic (PCA) reactions, an *in vivo* model of IgE-dependent mast cell degranulation, than $Kit^{W\text{-}sh}$ mice reconstituted with WT BMMCs. In the absence of 2-ME in culture, the mRNA expression of the anti-oxidative genes NF-E2-related factor 2 (*Nrf2)*, superoxide dismutase 2 (*SOD2)*, and heme oxygenase-1 (*HO-1)* was lower and reactive oxygen species (ROS) generation was higher in *Bmal1*-KO BMMCs than in WT BMMCs at steady state. The IgE-dependent ROS generation and degranulation were enhanced in *Bmal1*-KO BMMCs compared to WT BMMCs in the absence of 2-ME in culture. The addition of 2-ME into the culture abrogated or weakened the differences in anti-oxidative gene expression, ROS generation, and IgE-dependent degranulation between WT and *Bmal1*-KO BMMCs.

Conclusion

The current findings suggest that *Bmal1* controls the expression of anti-oxidative genes in mast cells and *Bmal1* deficiency enhanced IgE-dependent degranulation associated with promotion of ROS generation. Thus, *Bmal1* may function as a key molecule that integrates redox homeostasis and effector functions in mast cells.

Key words

Bmal1, mast cells, IgE, degranulation, ROS

1. Introduction

The circadian clock enables organisms to coordinates their behavior and physiological processes including metabolism and immunity in synchrony with the changing 24-hour environment [1]. In mammals, the circadian rhythms are generated by the interlocked transcriptional-translational feedback loops (TTFLs) consisting of core clock genes include *brain and muscle Arnt-like protein-1* (*Bmal1*), *circadian locomoter output cycles protein kaput (Clock)*, *Cryptochrome 1-3* (*Cry1-3*), and *Period 1* and *2* (*Per1, Per2*) [2,3]. Among the clock genes, *Bmal1* is a transcription factor that has a basic-helix-loop-helix (bHLH)/Per-Arnt-Sim (PAS) domain, is the only non-redundant gene since single knock out mice for *Bmal1* become immediately arrhythmic after their release into constant dark conditions whereas single knock out mice for *Clock*, *Cry1-3*, and *Per1,2* do not show such phenotypes [4]. Therefore, *Bmal1* appeares to have a prominent function within the circadian oscillator.

In the present study, we explored the roles of *Bmal1* in mast cell function, in particular, in IgE-dependent mast cell degranulation. Mast cells are granulated immune cells of the myeloid lineage found resident in tissues throughout the body, which is crucial for effector functions in allergic reactions [5.6]. Mast cells can be activated by a number of stimuli, but IgE is the best known mechanism to trigger their activation. Allergen cross-linking of the high affinity Fc receptor for IgE (FcεRI) on mast cells triggers their degranulation and releases a set of biochemical mediators, thereby recruiting and activating other leucocytes and leading to the development of allergic inflammation [7]. It is well established that the core clock proteins (BMAL1, CLOCK, and PERIOD1/2) are expressed by mast cells [8], and we and others have shown that mast cell activity follows a circadian rhythm [8-10]. However, the functional roles of *Bmal1* in mast cells remain to be determined. This study aimed to elucidate the specific roles of *Bmal1* in IgE-dependent mast cell degranulation using bone marrow–derived mast cells (BMMCs) derived from *Bmal1*-deficient mice (*Bmal1*-KO mice).

2. Materials and Methods

2.1. Mice

The breeders of *Bmal1*$^{+/-}$ mice [11] (stock No. 009100) on a C57BL/6J background were purchased from the Jackson Laboratory (Bar Harbor, ME, USA). *Bmal1*$^{+/-}$ mice were crossed with *Bmal1*$^{+/-}$ mice to obtain *Bmal1*$^{-/-}$ (KO) and *Bmal1*$^{+/+}$ (WT) littermates. Mast cell-deficient C57BL/6-*Kit*$^{W\text{-}sh}$ mice [12] were provided by the RIKEN Bio Resource Center through the National Bio-Resource Project of the MEXT/AMED (Tsukuba, Japan). Eight–twelve-week-old male mice were used for all experiments. All mice were housed for at least two weeks under 12-hour light/12-hours dark conditions with *ad libitum* access to food and water. All animal experiments were approved by the Institutional Review Board of the University of Yamanashi (No. A3-40).

2.2. Mast cell reconstitution

C57BL/6-*Kit*$^{W\text{-}sh}$ mice were reconstituted with subcutaneous injections of bone marrow-derived mast cells (BMMCs) (1.5×10^6/mouse) derived from WT or *Bmal1*-KO mice, as previously described [13]. Four weeks after reconstitution, 8 to 12-old male mice were used for all experiments.

2.3. Generation of bone marrow-derived mast cells (BMMCs).

BMMCs were generated from mice femoral bone marrow cells as previously described [13]. Briefly, sterile bone marrow was harvested from the mice femur and cultured in RPMI1640 supplemented with 10% FBS, 1% P/S, 1% sodium pyruvate, 1% non-essential amino acids (NEAAs), 10 μg/mL recombinant mouse IL-3 (Peprotech, USA) and with or without 0.1% 2-Mercaptoethanol (2-ME) (Thermo Fisher Gibco^{TM}, USA). After 6 weeks culture, mature (purity > 95% c-kit$^+$ FcεRIα$^+$) mast cells were identified by flow cytometric detection cell-surface c-kit (CD117) and FcεRIα.

2.4. FACS staining

BMMCs were incubated for 15 minutes with rat-anti-mouse Abs to CD16/32 (2.4G2; BD Biosciences, San Diego, CA) to block nonspecific binding, and then were stained with FITC-conjugated anti-mouse FcεRIα (MAR-1; eBioscience, CA) and a PE-conjugated anti-mouse c-Kit Ab (2B8; BD PharMingen, CA) in PBS. After being washed with PBS, the stained cells (live-gated on the basis of forward and side scatter profiles) were analyzed on a quantitated by BD AccuriTM C6 flow cytometry (Becton

Dickinson) and data were processed using the BD AccuriTM CFlow software program (Becton Dickinson).

2. 5. Mast cell morphology

Six to eight-week-cultured BMMCs morphology were evaluated by 0.05% Toluidine Blue Solution (pH 4.1, Fujifilm, Ohsaka, Japan), esterase staining kit (Naphthol AS-D Chloroacetate [Specific Esterase] Kit, Sigma-Aldrich)**,** and Diff-Quik staining (Polysciences, Inc., Tokyo, Japan) following manufactures instructions.

2.6. Quantitative real-time PCR.

Total RNA collected by RNeasy Mini kit (Qiagen, Netherlands). The cDNA) was synthesized from RNA samples by the ReverTra Ace^{TM} qPCR RT Master Mix with gDNA remover (TOYOBO, Japan). A quantitative real-time PCR analysis using cDNA from BMMCs were performed using the StepOneTM real-time PCR system (Applied Biosystems, CA) according to the manufacturer's instructions. Primers and probes of mouse c-kit, FcεR1α, FcεR1β, FcεR1γ, Syk, Lyn, GATA2, HDC, Mcpt5, Mcpt6, Nrf2, SOD2, HO-1, and GAPDH were purchased from Applied Biosystems, CA. The ratio of the indicated genes to that of GAPDH was calculated, and the relative expression levels are shown. To evaluate anti-oxidative gene expression, 2-ME supplemented or no-supplemented RPMI1640 medium-cultured BMMCs were stimulated by H_2O_2 (100 or 500 μM) for 6 hours before RNA collection.

2.7. β-Hexosaminidase release assay

The β-hexosaminidase release assay was performed as previously described [13]. Briefly, WT or *Bmal1*-KO mice-derived BMMCs were incubated with 1 μg/ml anti–TNP mouse IgE mAb for overnight at 37°C, and then stimulated with 1 μg/ml of anti-mouse IgE antibody for 40 minutes at 37°C. Total release was obtained by adding 1% Triton buffer for 40 minutes. The supernatants were collected from each well and mixed with *p*-nitrophenyl-*N*-acetyl-β-D-glucosaminide to determine the enzymatic activity of the released β-hexosaminidase. After 90 minutes at 37°C, the reaction was stopped by adding 0.2 M glycine solution, and measured by absorption spectrometer (at 405 nm). The percentage of β-hexosaminidase release was calculated as follows:
β-hexosaminidase release (%) = OD of stimulated supernatant/ OD of supernatant of Triton-lysed cells x100

2.8. Cell viability

For apoptosis cells detection, BMMCs (1×10^6 cells/ mL) were untreated or treated with H_2O_2 (100 or 500 μM) for 24 hours in the presence or absence of 2-ME and were evaluated by FACS using the FITC conjugated-Annexin V Apoptosis Detection Kit (DOJINDO LABORATORIES, Kumamoto, Japan), following the manufacturer's instructions.

2.9. Reactive oxygen species (ROS) detection

BMMCs cultured in the presence or absence of 2-ME in RPMI1640 medium were sub-cultured at 1 x 10^6 cells per well. After 24 hours, BMMCs were stained with 5 μM CellROX™ Green Reagent (Invitrogen™, Thermo Fisher Science, Waltham, MA, USA) for 30 minutes at 37℃ according manufacturers instruction. The cells were washed in PBS and analyzed using a AccuriTM C6 flow cytometry. For detection of ROS production in BMMCs after IgE-dependent degranulation, BMMCs were stained with CellROX™ green 1 hour after stimulation with anti-IgE.

2.10. Passive cutaneous anaphylaxis (PCA) reaction in the ear of WT and *Bmal1*-KO mice

PCA reaction in ear was performed as previously described [14]. Briefly, one side of mouse ear was intradermally sensitized with anti-TNP mouse IgE (100 ng/10 μL/ear), whereas the other side mouse ear was intradermally administrated PBS as negative control. Twenty-four hours later, mice were intravenous administrated TNP-BSA (50 μg/200 μL)/0.2% Evans blue dye mixture. Ear thickness was measured before the TNP-BSA challenge (0 minutes) and then at 15, 30, 60, 90, and 180 minutes. Increased-ear thickness was determined by deducting the ear thickness value at 0 minutes from every time point of ear thickness. After 180 minutes, blood samples were collected to evaluated serum MCP-1 (CCL2) levels by mouse CCl2/JE/MCP-1 Quantikine ELISA Kit (R & D Systems Inc. Minneapolis, MN). To evaluate Evans blue dye extravasation in the ear, mice ear were collected after 180 minutes PCA induction. Chopped into small pieces of the ear were mixed with N, N-Dimethylformamide solution and incubated for 3 hours at 55℃. Supernatant were collected and measure absorbance value with 650 nm filter.

2.11. Toluidine blue staining

Mast cell numbers in the back skin of WT or *Bmal1*-KO mice were evaluated by toluidine blue staining before the induction of PCA reaction. The collected back skin

samples were fixed with 4% paraformaldehyde and paraffin-embedded, after which 10 μm sections were prepared. The sliced samples were stained with 0.1% Toluidine blue (pH 4.1) and the numbers of mast cells were quantified by microscopy.

2.12. PCA reaction in the back skin of mast cell-reconstituted mice

Induction of PCA reaction in the back skin of WT or *Bmal1*-KO BMMCs (1.5 x 10^6 cells/mouse)-reconstituted C57BL/6-*Kit*$^{W\text{-}sh}$ mice were performed as previously described [13]. Briefly, mice were sensitized via subcutaneous injection of anti-TNP mouse IgE (0.5 μg/20 μL, BD Bioscience, USA). The mice were then challenged intravenous injection 24 hours later with 50 μg of TNP-BSA (Cosmo Bio, Tokyo, Japan) with 0.2% Evans blue dye. Vascular permeability was visualized 30 minutes later by the blue staining of the injection sites on the reverse side of the skin. These staining sites were digitalized using a high-resolution color camera (digital cameraIXY3, Canon Inc., Tokyo, Japan) and the images were saved in Windows photo viewer as 8-bit color-scale JPEG files. The open source ImageJ 1.43 software package (NIH, USA) was used for the image analysis. The color-scale images exported from Windows photo viewer were converted to HSB ("hue/saturation/brightness") stack type images using the Image tool. Thereafter, the HSB stack images were split into hue, saturation, and brightness images, respectively. Only blue color stained-areas were selected from the hue image using the threshold tool. These images were then combined with the saturation image and the density values for the blue color stained-areas, and were measured using the analyze tool.

2.13. Statistics

Data analysis was performed using GraphPad Prism 8 (GraphPad software Inc., MA). Results are expressed as mean ± SD and the "n" numbers for each dataset are provided in the figure legends. Statistical significance was assessed by two-tailed Student's t test, one-way followed by Dunnett's, Tukey's post-hoc test or two-way ANOVA followed by Tukey's. P values <0.05 (shown as *P<0.05, **P<0.01, ***P<0.001 or ****P<0.0001) were considered significant.

3. Results and Discussion

Firstly, we determined whether Bmal1 deficiency could affect mast cell differentiation. By 6 weeks of culture, both WT and *Bmal1*-KO BMMC cultures contained >90% of KIT and FcεRIα double-positive cells (**Fig. 1A**). Surface c-kit and FcεRIα expression levels were comparable between WT and *Bmal1*-KO BMMCs (**Fig. 1B**). WT and *Bmal1*-KO BMMCs showed similar morphology, as determined by toluidine blue, esterase, and Diff Quik staining (**Fig. 1C–E**). The mRNA expression of mast cell differentiation marker genes encoding granule proteases, such as *Mcpt5* and *6*; mast cell lineage–determining transcription factor *GATA2* [15]; histidine decarboxylase (*HDC*); and signaling molecules involved in FcεRI signaling, such as *FcεRIα*, *FcεRIβ*, *FcεRIγ*, *Lyn*, and *Syk*, was comparable between WT and *Bmal1*-KO BMMCs **(Fig. 1F)**. The presence or absence of 2-ME in culture did not affect these parameters (**Fig. 1-F, data not shown**). These findings indicate that cell differentiation and morphology did not differ significantly between WT and *Bmal1*-KO BMMCs.

Interestingly, we found that IgE-dependent degranulation was more robust in *Bmal1*-KO BMMCs than in WT BMMCs in the absence of 2-ME in culture, as determined by the β-hexosaminidase release assay (**Fig. 2A**). The extent of passive cutaneous anaphylaxis (PCA) reactions in *Bmal1*-KO mice was also more robust than those in WT mice, as determined by the ear thickness, evans blue dye quantification, and serum CCL2 levels **(Fig. 2B)**. We confirmed that the number of mast cells in mouse back skin was comparable between WT and *Bmal1*-KO mice, as determined by toluidine blue staining (**Fig. 2C**). Furthermore, mast cell–deficient $Kit^{W\text{-}sh}$ mice reconstituted with *Bmal1*-KO BMMCs showed more robust PCA reactions than $Kit^{W\text{-}sh}$ mice reconstituted with WT BMMCs, as determined by the quantification of evans blue dye-staining areas digitized using a high-resolution camera (**Fig. 2D**). These results suggest that deficiency of *Bmal1* enhances IgE-dependent degranulation in mast cells both *in vitro* and *in vivo*.

Next, we explored possible mechanisms underlying the enhanced response to IgE in *Bmal1*-deficient mast cells. *Bmal1* is crucial for anti-oxidative responses in different tissues and cells [16]. In addition, reactive oxygen species (ROS) are involved in intracellular signaling induced by FcεRI aggregation and are required for degranulation [17]. Therefore, we examined whether Bmal1 is involved in the anti-oxidative response in mast cells.

In the absence of 2-ME in culture, the mRNA expression of the anti-oxidative genes NF-E2-related factor 2 (*Nrf2)*, superoxide dismutase 2 (*SOD2)*, and heme

oxygenase-1 (*HO-1)* was lower and ROS generation was higher in *Bmal1*-KO BMMCs than in WT BMMCs at steady state (**Fig. 3A and B**). Exposure to H_2O_2 increased apoptosis of *Bmal1*-KO BMMCs compared with WT BMMCs in the absence of 2-ME in culture (**Fig. 3C**), which was associated with enhanced ROS generation (**Fig. 3D**) and impaired *Nrf2* and *SOD2* mRNA induction (**Fig. 3E**). FcεRI aggregation induced ROS generation in WT BMMCs as previously described [17] and this effect was enhanced in *Bmal1*-KO BMMCs in the absence of 2-ME in culture (**Fig. 3F**). Importantly, the addition of 2-ME into the culture abrogated or weakened the significant differences in anti-oxidative gene expression, ROS generation, H_2O_2-induced apoptosis, and IgE-dependent degranulation between WT and *Bmal1*-KO BMMCs (**Fig. 2A, Fig. 3**). These results suggest that *Bmal1* controls the expression of anti-oxidative genes in mast cells, and *Bmal1* deficiency promotes ROS generation, associated with increased sensitivity to H_2O_2 and enhanced IgE-dependent degranulation.

The circadian clock regulates the expression and activity of mitochondrial anti-oxidant enzymes and redox homeostasis in several tissues [16]. For instance, *Bmal1* expression levels in hepatocytes were negatively correlated with elevated ROS accumulation in mice with metabolic-associated fatty liver disease [18]. This study suggests that this is also the case in mast cells, which is linked to enhanced IgE-dependent degranulation (**Fig. 2 and Fig. 3**). Thus, the current results uncover a role for *Bmal1* in regulating anti-oxidative responses in mast cells to control IgE-dependent degranulation.

The present findings additionally showed that 2-ME in cell culture could have significant impact on intracellular ROS generation and IgE-dependent degranulation in mast cells. It remains unclear whether this observation is specific to mast cells, but the results suggest that we should be cautious to evaluate cellular physiological outputs in the presence of 2-ME in *in vitro* cell culture system since 2-ME can affect intracellular ROS levels.

In summary, this study addressed the role of the core clock component *Bmal1* in IgE-dependent degranulation in mast cells, which is central to the pathophysiology of allergic diseases. We found that *Bmal1* deletion in mast cells enhanced IgE-dependent degranulation both *in vitro* and *in vivo*, associated with increased ROS generation. Thus, *Bmal1* may function as a key molecule that integrates redox homeostasis and effector functions in mast cells. The findings also implicate that the disruption of circadian clock activity (*e.g.*, *Bmal1* rhythmic expression) could worsen symptoms in IgE/mast cell–mediated allergic diseases.

Declarations

Ethical approval

All animal experiments were approved by the Institutional Review Board of the University of Yamanashi (No. A3-40).

Competing interests

The authors have no conflicts of interest to declare.

Authors' contributions

Yuka N, Yuki N, and AN designed the study. Yuka N, Yuki N, NQVT, YK, and NN collected and analyzed the data. Yuka N, Yuki N, and AN wrote the manuscript.

Funding

This research was funded by a grant-in-aid for scientific research to AN from the Ministry of Education, Culture, Sports, Science, and Technology, Japan (grant number 22K19427).

Acknowledgement

We thank Ms. Yukino Fukasawa, Ms. Tomoko Tohno, and Ms. Maiko Aihara for their excellent assistance.

Availability of data and materials

The data and materials are available from the corresponding author on reasonable requests.

References

[1] Turek FW. Circadian clocks: Not your grandfather's clock. *Science.* 354 (2016) 992-993. htttps:// doi: 10.1126/science.aal2613.

[2] Takahashi JS. Transcriptional architecture of the mammalian circadian clock. *Nat Rev Genet*. 18 (2017)164-179. https:// doi: 10.1038/nrg.2016.150.

[3] Patke A, Young MW, Axelrod S. Molecular mechanisms and physiological importance of circadian rhythms. *Nat Rev Mol Cell Biol.* 21 (2020) 67-84. https:// doi: 10.1038/s41580-019-0179-2.

[4] Ripperger JA, Jud C, Albrecht U. The daily rhythm of mice. *FEBS Letters.* 585 (2011) 1384-1392. https:// doi: 10.1016/j.febslet.2011.02.027.

[5] Levi-Schaffer F, Gibbs BF, Hallgren J, Pucillo C, Redegeld F, Siebenhaar F, et al. Selected recent advances in understanding the role of human mast cells in health and disease. *J Allergy Clin Immunol.* 149 (2022)1833–1844. https:// doi: 10.1016/j.jaci.2022.01.030.

[6] Galli SJ, Gaudenzio N, Tsai M. Mast Cells in Inflammation and Disease: Recent Progress and Ongoing Concerns. *Annu Rev Immunol.* 38 (2020) 49-77. https:// doi: 10.1146/annurev-immunol-071719-094903.

[7] Blank U, Huang H, Kawakami T. The high affinity IgE receptor: a signaling update. *Curr Opin Immunol.* 72 (2021) 51–58. https:// doi: 10.1016/j.coi.2021.03.015.

[8] Wang X, Reece SP, Van Scott MR, Brown JM. A circadian clock in murine bone marrow-derived mast cells modulates IgE-dependent activation in vitro. *Brain Behav Immun.* 25 (2011) 127-134. https:// doi: 10.1016/j.bbi.2010.09.007.

[9] Christ P, Sowa AS, Froy O, Lorentz A.
The Circadian Clock Drives Mast Cell Functions in Allergic Reactions. *Front Immunol.* 9 (2018) 1526. https:// doi: 10.3389/fimmu.2018.01526.

[10] Nakao A, Nakamura Y. Time will tell about mast cells: Circadian control of mast cell activation. *Allergol Int.* 71 (2022) 425-431. https://doi: 10.1016/j.alit.2022.06.008.

[11], Moran SM, Clendenin C, Radcliffe LA, Hogenesch JB, Simon MC, Takahashi JS, Bradfield CA. Mop3 is an essential component of the master circadian pacemaker in mammals. *Cell.* 103 (2000) 1009-1017. https://doi: 10.1016/s0092-8674(00)00205-1.

[12] Grimbaldeston MA, Chen CC, Piliponsky AM, Tsai M, Tam SY, Galli SJ. Mast cell-deficient W-sash c-kit mutant Kit W-sh/W-sh mice as a model for investigating mast cell biology in vivo. *Am J Pathol.* 167 (2005) 835-848. https:// doi: 10.1016/S0002-9440(10)62055-X

[13] Nakamura Y, Nakano N, Ishimaru K, Hara M, Ikegami T, Tahara Y, et al. Circadian regulation of allergic reactions by the mast cell clock in mice. *J Allergy Clin Immunol.* 133 (2014) 568-575. https:// doi: 10.1016/j.jaci.2013.07.040.
[14] Giménez-Rivera VA, Metz M, Siebenhaar F. Mast cell-mediated reactions *in vivo*. *Methods Mol Biol.* 1192 (2014) 239-247. https:// doi: 10.1007/978-1-4939-1173-8_18
[15] Derakhshan T, Boyce JA, Dwyer DF. Defining mast cell differentiation and heterogeneity through single-celltranscriptomics analysis. *J Allergy Clin Immunol.* 150 (2022) 739-747. https:// doi: 10.1016/j.jaci.2022.08.011
[16] Hardeland R, Coto-Montes A, Poeggeler B. Circadian rhythms, oxidative stress, and antioxidative defense mechanisms. *Chronobiol Int.* 20 (2003) 921-962. https://doi: 10.1081/cbi-120025245.
[17] Chelombitko MA, Fedorov AV, Ilyinskaya OP, Zinovkin RA, Chernyak BV. Role of Reactive Oxygen Species in Mast Cell Degranulation. *Biochemistry* (Mosc). 81 (2016) 1564-1577. https://doi: 10.1134/S000629791612018X.
[18] Ye C, Zhang Y, Lin S, Chen Y, Wang Z, Feng H, Fang G, Quan S. Berberine Ameliorates Metabolic-Associated Fatty Liver Disease Mediated Metabolism Disorder and Redox Homeostasis by Upregulating Clock Genes: Clock and Bmal1 Expressions.
Molecules. 28 (2023) 1874. https://doi: 10.3390/molecules28041874.

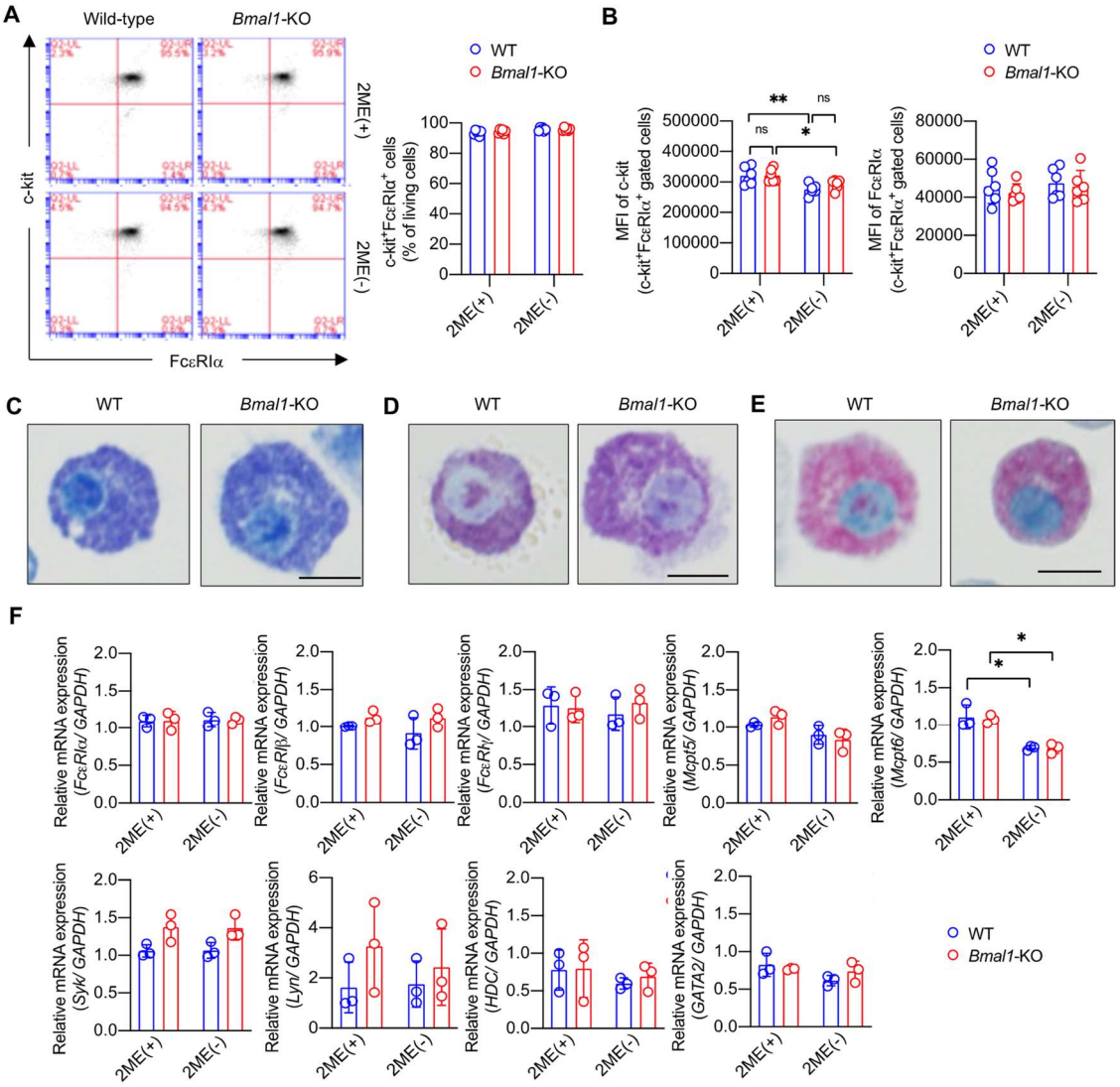

Figure 1

Bmal1 deficiency does not affect differentiation and morphology of BMMCs.

(A) Representative dot-plot data (**Left**) and percentage of c-kit^{+}FceRIa^{+} cells (**Right, n=6**) of WT or *Bmal1-KO* BMMCs cultured in the presence or absence of 2-ME after 6-8 weeks detected by flowcytometric analysis.

(B) Flowcytometric analysis of mean fluorescence intensity (MFI) of c-kit (**Left**) or FceR1a levels (**Right**) of WT or *Bmal1-KO* BMMCs cultured in the presence or absence of 2-ME after 6-8 weeks (n=6).

(C-E) Representative pictures of toluidine blue (**C**), Diff-Quik (**D**) or esterase (**E**) staining of WT or *Bmal1-KO* BMMCs cultured in the presence of 2-ME after 6-8 weeks.

(F) Expression of mast cell differentiation marker and functional genes, determined by qPCR in WT or *Bmal1*-KO BMMCs cultured in the presence or absence of 2-ME for 6-8 weeks (n=3).
Mean ± SD is shown. Statistical differences were determined by two-way ANOVA with Tukey's post hoc test, *P<0.05. ns: non-specific difference.

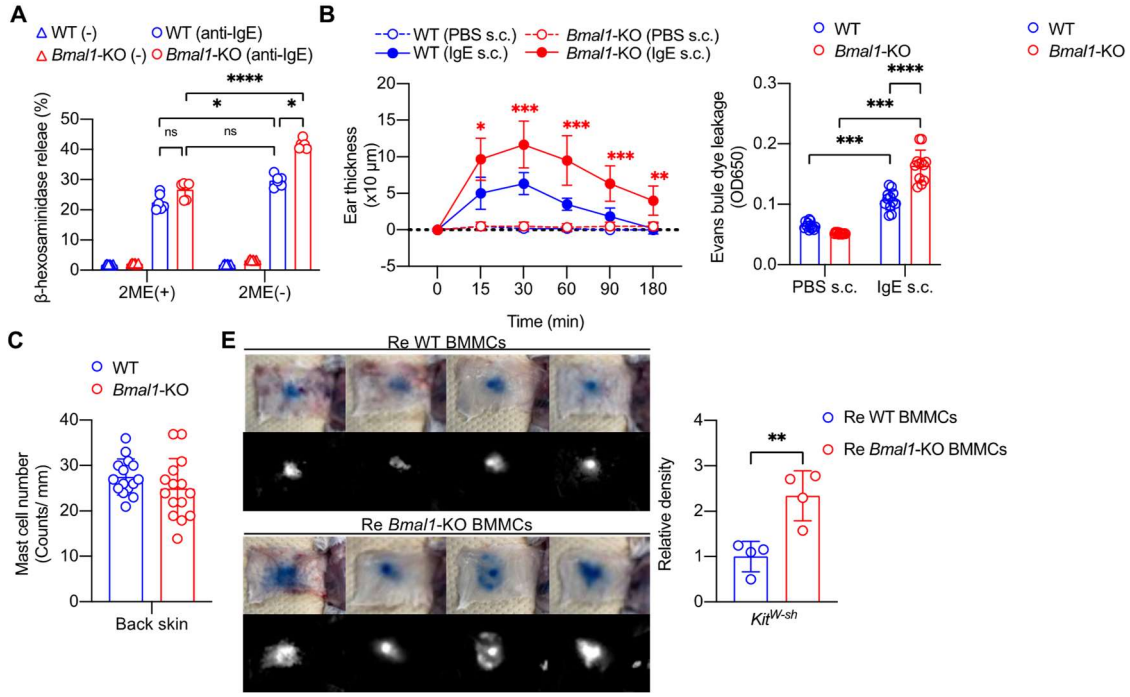

Figure 2

Deficiency of *Bmal1* enhances IgE-dependent degranulation in mast cells both *in vitro* and i*n vivo.*

(A) IgE-dependent degranulation as determined by the β-hexosaminidase release assay in WT or *Bmal1-KO* BMMCs cultured in the presence or absence of 2-ME for 6-8 weeks (n=6).

(B) Kinetics of ear thickness after induction of PCA reaction in WT or *Bmal1-KO* mice (**Left**, n=6). Evans blue extravasation in the ear (**Middle**, n=12) or serum CCL2 levels (**Right**, n=6) at 180 minutes after the induction of PCA reaction.

(C) The number of toluidine blue dye-stained mast cells in the back skin of WT or *Bmal1-KO* mice (n=15).

(D) (**Left**) Representative images of PCA reaction in mast cell-deficient $Kit^{W\text{-}sh}$ mice reconstituted with subcutaneous injections of WT BMMCs or *Bmal1-KO* BMMCs**.** Color images are the real pictures of PCA reaction and black/white images are digitized images used for the density value evaluations. **(Right)** Quantitative analysis of the digitized images of the PCA reaction (n=4).

Mean ± SD is shown. Statistical differences were determined by two-tails unpaired student's T-test (**D**) or two-way ANOVA with Tukey's post hoc test(**A-C**), *P<0.05, **P<0.01, ***P<0.001, ****P<0.0001.

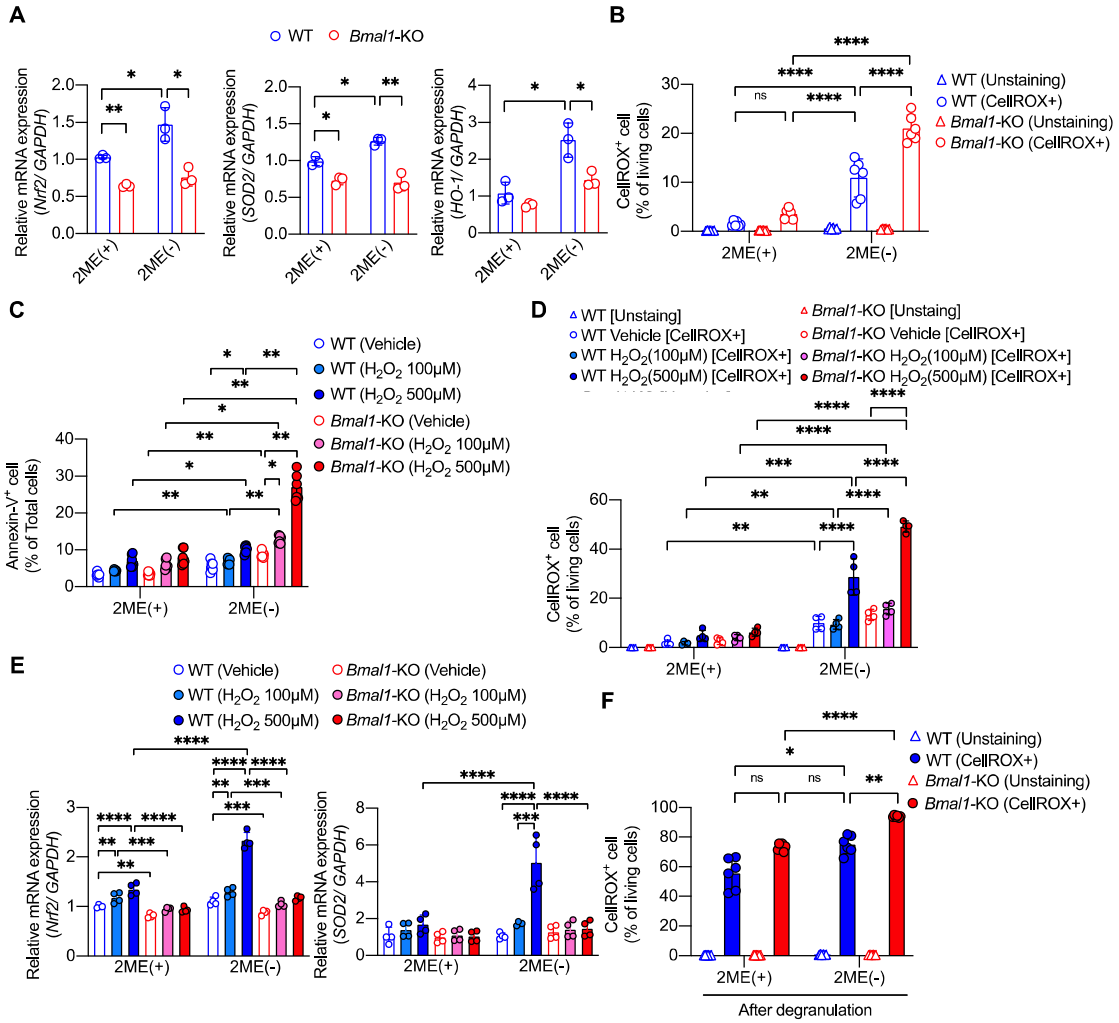

Figure 3

***Bmal1* deficiency decreases expression of anti-oxidative genes and promotes ROS generation in mast cells.**

WT or *Bmal1-KO* BMMCs were cultured in the presence or absence of 2-ME for 6-8 weeks (**A-F**).

(A) Anti-oxidative genes expression of WT or *Bmal1-KO* BMMCs detected by qPCR (n=3).

(B) ROS generation in WT or *Bmal1-KO* BMMCs at steady state detected by flowcytometric analysis (n=6).

(C) Annexin-V$^+$ apoptosis cells of WT or *Bmal1-KO* BMMCs after stimulation with H_2O_2 (100 or 500 μM) for 24 hours detected by flowcytometric analysis (n=6).

(D) ROS generation after stimulation of H_2O_2 (100 or 500 μM) for 2 hours in WT or *Bmal1-KO* BMMCs by flowcytometric analysis (n=6).

(E) Anti-oxidative genes expression after stimulation with H_2O_2 (100 or 500 μM) for 6 hours in WT or *Bmal1-KO* BMMCs detected by qPCR (n=4).
(F) ROS generation after the stimulation with IgE in WT or *Bmal1-KO* BMMCs for 1 hour detected by flowcytometric analysis (n=6).
Mean ± SD is shown. Statistical differences were determined by one-way ANOVA with Dunnett's post hoc test or two-way ANOVA with Tukey's post hoc test, *P<0.05, **P<0.01, ***P<0.001, ****P<0.0001. ns: non-specific difference.